

Strength and reliability analysis of MEMS micromirror

Chan Wee Ping , Satoshi IZUMI, Shinsuke SAKAI

Keywords: MEMS micromirror, combined loading, load factor analysis, Weibull plot, Bayesian reliability analysis

1. Research background

MEMS micro-mirrors have been widely used in optical switches and scanning devices⁽¹⁾. In these kinds of applications, the beams supporting the micro mirror are twisted and deformed to a large extent. Consequently, these beams failed by brittle fracture catastrophically. Hence, there is a need to clarify the mechanical characteristics of such beams.

Until now, many researches have been performed to determine the mechanical properties of MEMS. However, most of them are pure bending tests or direct tensile tests. As a result, the fracture strength determined through such tests is associated with bending or tensile fracture. On the other hand, fractures due to torsional loading are not well documented. Hence, there is still much room for research relating to torsional fractures.

2. Aims of research

The aim of this research is to design a specimen for micro testing and propose an experimental procedure for micro testing. Next, pure bending and combined (torsion and bending) loading test will be performed on the samples. Then a fracture criterion based on the experimental data will be proposed. Finally, a general safety design criterion for microstructure under torsional loading will be proposed.

3. Design of specimen for micro testing

Since it is almost impossible to perform a pure torsional test, combined loading will be performed and the effect of pure torsional loading will be estimated based on load factor analysis. A number of factors have to be considered when designing a specimen for micro testing.

Firstly, the experimental constraints. The load cell has a maximum capacity of 5N and the applied load can be measured to within $\pm 1\%$ of its value. The range of the LDM (laser displacement meter) is 1mm and its accuracy is 0.5 μ m. Here, the slowest testing speed of 0.5mm/min is used in order to get the maximum number of sampling results. Next, the rotational angle cannot be too large or slippage of the loading needle may occur. Moreover, if the rotation angle is too large, curvature shortening may lead to unwanted tensile forces acting on the beams. The maximum rotational angle is preferably taken to be 30deg. In the design process, the center deflection is taken to be in the order of 0.1mm and the edge deflection in the order of 1mm.

Secondly, it has to be ensured that the specimen fails under torsional loading. The shear stress due to torsion can be expressed as a function of a , b , θ , L and G (Refer to Fig. 1) The normal stress due to flexure can be expressed as a function of a , b , c , d , θ , L and G . When the ratio of the shear stress to the normal stress is taken, θ and G are being cancelled out. Thus the stress ratio (ratio of maximum shear stress to maximum normal stress, irrespective of location in the beam) depends on a , b , c , d and L .

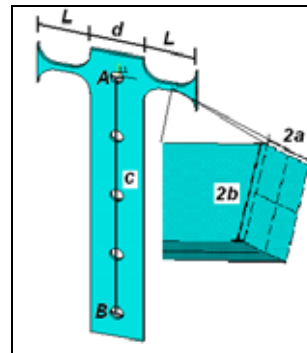
The final dimensions of the beam are as follow: $2a=150\mu\text{m}$; $2b=240$ and $300\mu\text{m}$; $c=10\text{mm}$; $d=2\text{mm}$ and $L=2\text{mm}$. When a force is 5N at applied at $c=10\text{mm}$, a stress ratio of about 6 is obtained, with the maximum shear stress being about 2.45GPa.

4. Experimental procedure

4-inch (100)-oriented 150/1/400 μ m thick SOI wafers were used. Bulking silicon micromachining was performed by means of the ICP-RIE equipment from Sumitomo Precision Products.

For the experiment, the 'EZ TEST' testing machine from Shimadzu Corporation and the 'LC-2400' LDM from Keyence Corporation were used.

Firstly, pure bending was performed by applying the force at location A shown in Fig. 1. Both the force and displacement up to the point of fracture were recorded and then used to derive the approximate maximum principal stress in the beam at the point of fracture. Next, combined loading test will be performed by applying force at locations away from the mid-point of the plate, for instance at location B shown in Fig. 1.



2a: Height of beam
2b: Width of beam
c: Length of plate
d: Width of plate
L: Length of beam
 θ : Rotational angle
G: Shear modulus

A: Midpoint of plate
B: Edge of plate (at a distance of c from A)

Fig. 1: Dimensions of the beam

6. Pure bending and combined loading testing

A total of 74 samples were investigated for their bending and combined loading. (19 samples: 240 μ m and 300 μ m pure bending; 27 samples: 240 μ m combined loading and 28 samples: 300 μ m combined loading) A two-parameter Weibull plot for the ultimate normal stresses (nominal stresses) was shown in Fig. 2. The Weibull parameters were obtained using the maximum likelihood method and the results are shown in Table 1.

Both anisotropic material constant and geometric non-linearity have been considered in the FEM model, which was constructed using ANSYS6.0. Quadratic Shell 93 elements were used to construct the coarse model while hexahedron Solid 95 elements were used in the submodel.

Table 1: MLM estimation of Weibull parameters

	Scale Parameter	Weibull modulus
(240 μ m; 300 μ m) pure bending	783	7.77
240 μ m combined loading	517	5.28
300 μ m combined loading	306	4.98

5. Explanations for differences in strength and fractured criterion

From the Weibull plot in Fig. 2, it can be observed that (240 μ m; 300 μ m) pure bending samples were the strongest, followed by 240 μ m combined loading and 300 μ m combined loading. The difference in fracture strength between the samples could be explained using load factor analysis. The load factor (refer to equation (1) below) is an intrinsic characteristic for a specific geometry and loading configuration, independent of the fractured stress. Here, the load factor PDF (probability density function) or load factor index was proposed and calculated by numerical differentiation of the load factor. A higher load factor index would correspond to a more severe stress environment.

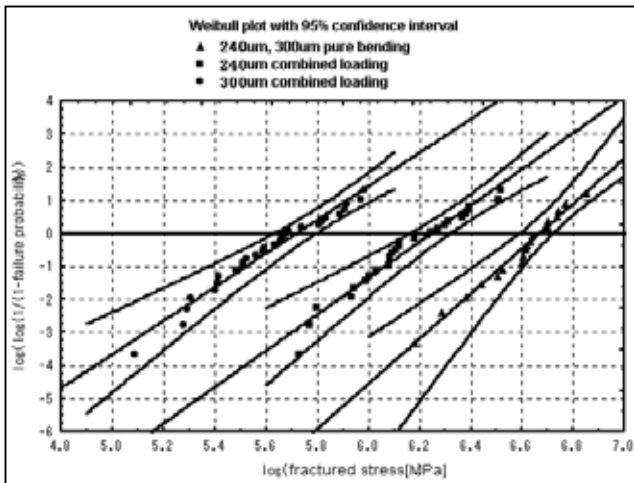


Fig. 2: Weibull plot of the ultimate normal stresses (nominal stresses)

$$\text{load factor} = \frac{1}{\text{volume}_{\text{region}}} \iiint (f(x, y, z))^m dx dy dz \quad (1)$$

whereby $f(x, y, z) = \frac{\sigma(x, y, z)}{\sigma_{\text{nominal}}}$ is the position function and m is the Weibull modulus. $\sigma(x, y, z)$ is the stress at a particular location and σ_{nominal} is the maximum stress in the region of concern. In this research, a line flaw along the edge of the beam was assumed because the flaws were observed to be concentrated along the beam edge as shown in Fig. 3. The difference in strength between pure bending and combined loading could be explained by the greater load factor index in the case of combined loading. Another possible reason was that for the case of combined loading, the direction of the maximum principal stress was more aligned with the general flaw direction. For instance, load factor values for 240um pure bending and 240um combined loading were 0.0687 and 0.319 respectively.

A separate fracture criterion was needed for each form of geometry and loading. Moreover, the fracture criterion proposed was in the form of PDF whose parameters were estimated from experimental data. Fracture criterion appropriate for combined loading could also be applied for the case of pure torsional loading since the combined loading had a higher overall load factor index and hence faced a more severe stress environment.

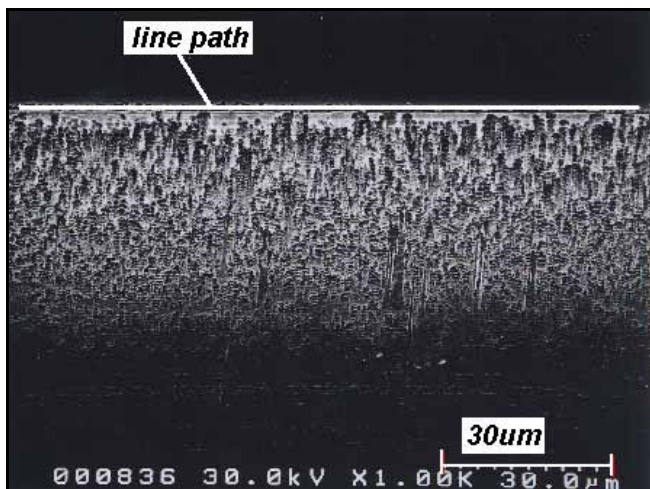


Fig. 3: Illustration of line path for load factor analysis

7. Fractography

The fractured surfaces were examined using the SEM. A typical fractured surface for the case of pure bending is shown in Fig. 4.

Initiation site occurred at the etching surface, which contained lots of micro-defects. Fracture surface was smooth near the initiation site (mirror), and rough and wavy away from the initiation site (mist). The mode of fracture was most probably Mode I. The direction of fracture was mostly at an angle to (110) plane; only a few were in the (110) plane. Size of defects was estimated to be in the region of 1um. A rough estimation using the Griffith criterion gave the nominal fracture stress of about 500MPa to 600MPa.

For the case of combined loading, undulating (mixed Mode I and II) and river patterns (mixed Mode I and III) could be observed, pointing to the existence of mixed-mode crack propagation.

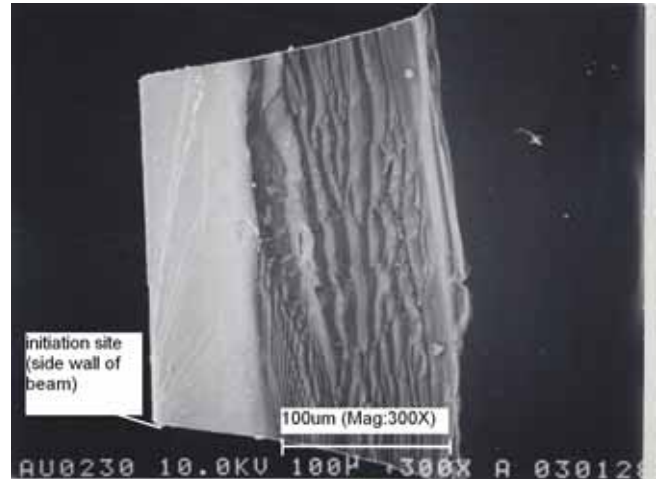


Fig. 4: A typical fractured surface for pure bending.

8. Reliability analysis

A general safety design criterion (not limited to the case of pure torsion loading) based on Bayesian reliability analysis was proposed. In the limiting case when there are an infinite number of samples, both the maximum likelihood method and Bayesian method will give the same estimate for the unknown parameters. In the case of finite samples, the two methods will give different estimates for the unknown parameters. The question arises as to which method is better. When there are very few samples, the Bayesian method is preferred. It is best that there is a prior knowledge of the PDF of the unknown parameters, which will result in better posterior PDF for the unknown parameters. Nevertheless, even if there is no expert opinion for the prior PDF, non-informative PDF for the unknown parameters can be used. Moreover, when there are major changes in the geometry, etching conditions and loading conditions, there is a need to redesign and re-perform the experiments. However, by using Bayesian reliability, which capitalizes on past data, number of samples needed for experiments can be kept to a bare minimum and much product developmental cost can be saved.

9. Conclusions:

Specimen suitable for micro testing has been designed and an experimental procedure for pure bending and combined loading have been proposed. Pure bending and combined loading tests have been performed. A separate fracture criterion for each form of geometry and loading has been proposed. Besides, fracture criterion for combined loading can be used for pure torsion loading based on load factor analysis. Finally, a general safety design procedure based on Bayesian reliability analysis has been proposed.

Reference:

- (1) N. Asada, H. Matsuki, K. Minami, M. Esashi, "Silicon Micromachined Two-Dimensional Galvano optical Scanner", IEEE Transactions on Magnetics, Vol.30, No. 6, Nov. 1994

